INTERFACE SCIENCE 12, 147–155, 2004

Grain Boundary Phase Transitions and their Influence on Properties of Polycrystals

B. STRAUMAL
Institute of Solid State Physics, Russian Academy of Sciences, Chernogolovka, Moscow district, 142432 Russia
straumal@issp.ac.ru; straumal@song.ru

B. BARETZKY
Max-Planck-Institut für Metallforschung, Heisenbergstr. 3, 70569 Stuttgart, Germany

Abstract. Grain boundary (GB) phase transitions can change drastically the properties of polycrystals. The GB wetting phase transition can occur in the two-phase area of the bulk phase diagram where the liquid (L) and solid (S) phases are in equlibrium. Above the temperature of the GB wetting phase transition a GB cannot exist in equlibrium contact with the liquid phase. The experimental data on GB wetting phase transitions in numerous systems are analysed. The GB wetting tie-line can continue in the one-phase area of the bulk phase diagram as a GB solidus line. This line represents the GB premelting or prewetting phase transitions. The GB properties change drastically when GB solidus line is crossed by a change in the temperature or concentration. The experimental data on GB segregation, energy, mobility and diffusivity obtained in various systems both in polycrystals and bicrystals are analysed. In case if two solid phases are in equilibrium, the GB "solid state wetting" can occur. In this case the layer of the solid phase 2 has to substitute GBs in the solid phase 1. Such GB phase transition occurs if the energy of two interphase boundaries is lower than the GB energy in the phase 1.

Keywords: grain boundaries, phase transitions, diffusion, segregation, energy, grooving

Introduction

The properties of modern materials, especially those of superplastic, nanocrystalline or composite materials, depend critically on the properties of internal interfaces such as grain boundaries (GBs) and interphase boundaries (IBs). All processes which can change the properties of GBs and IBs affect drastically the behaviour of polycrystalline metals and ceramics [1]. GB phase transitions are one of the important examples of such processes [2]. Recently, the lines of GB phase transitions began to appear in the traditional bulk phase diagrams [2–7]. The addition of these equilibrium lines to the bulk phase diagrams ensures an adequate description of polycrystalline materials. In this work GB wetting, prewetting and premelting phase transitions are reviewed. The GB melting, GB faceting transition and the "special GB—random GB phase transitions" are analyzed elsewhere [8–10].

Grain Boundary Wetting Phase Transitions

One of the most important GB phase transitions is the *GB wetting transition*. Since their prediction by Cahn [11] the study of wetting phase transitions has been of great experimental and theoretical interest, primarily for planar solid substrates and fluid mixtures [12–14]. Particularly, it was experimentally shown that the wetting transition is of first order, namely the discontinuity of the fisrt derivative in temperature dependence of the surface energy was measured and the hysteresis of the wetting behavior was observed [15, 16]. The important difference is that in case of GB wetting only two phases coexist, namely the liquid (melt) phase and the

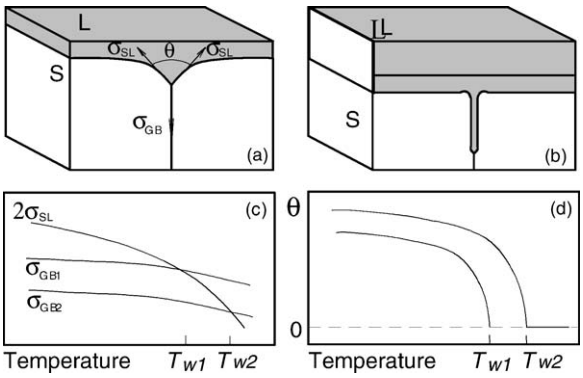

Figure 1. (a) Scheme of the equilibrium contact between the grain boundary in the solid phase S and the liquid phase L (incomplete wetting). (b) Complete GB wetting. (c) Scheme of the temperature dependence for the GB energy σ_{GB} (for two different GBs) and the energy of the solid-liquid interface boundary σ_{SL}. (d) Scheme of the temperature dependence of the contact angle θ for two grain boundaries with energies σ_{GB1} and σ_{GB2}. T_{w1} and T_{w2} are the temperatures of the GB wetting phase transition.

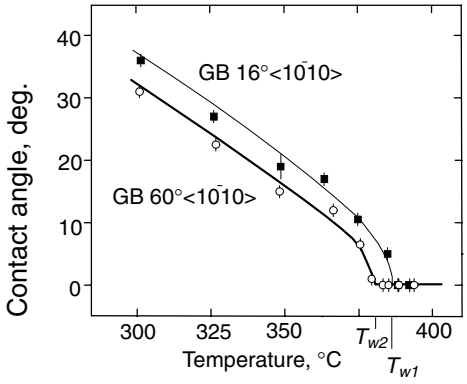

Figure 2. Temperature dependences of the contact angle between Sn-rich melt and two tilt GBs in Zn 16°[1, 0, −1, 0]($T_w = 386.5 + 1$°C) and 60°[1, 0, −1, 0]($T_w = 381 + 1$°C) [7].

solid one containing the boundary between the misoriented grains. Therefore, the contact angle θ also depends only on two different surface energies (the GB energy σ_{GB} and the energy of the solid/liquid interphase boundary σ_{SL}) $\sigma_{GB} = 2\sigma_{SL}\cos(\theta/2)$. In usual experiments three surface energies (solid/liquid, solid/gas and gas/liquid) define the contact angles. If $\sigma_{GB} < 2\sigma_{SL}$, the GB is incompletely wetted and the contact angle $\theta > 0$ (Fig. 1(a)). At the temperature T_w of the *GB wetting phase transition* $\sigma_{GB} = 2\sigma_{SL}$, and at $T \geq T_w$ the GB is completely wetted by the liquid phase and $\theta = 0$ (Fig. 1(b)). The contact angle θ decreases gradually with increasing temperature down to zero at T_w (see also the Fig. 2 for the system Zn–Sn). At $T > T_w$ the contact angle $\theta = 0$ (Figs. 1(d) and 2). If two GBs have different energies the temperatures of their GB wetting transitions will also differ: the lower σ_{GB}, the higher T_w (Fig. 1(c) and (d)). If the GB wetting phase transition is of first order, there is a discontinuity of first derivative in temperature dependence of the Gibbsian energy of the interface/interfaces separating two adjacent grains at T_w which is equal to $[\partial\sigma_{GB}/\partial T - \partial(2\sigma_{SL})/\partial T]$ [11, 16]. If the GB wetting phase transition is of second order, $\partial\sigma_{GB}/\partial T = \partial(2\sigma_{SL})/\partial T$ at T_w. The theory predicts also the shape of the temperature dependence $\theta(T)$ at $T \to T_w$: it must be convex for a first order wetting transition [$\theta \sim \tau^{1/2}$ where $\tau = (T_w - T)/T_w$] and concave for a second order wetting transition: $\theta \sim \tau^{3/2}$ [12].

Nowdays, the GB phase transitions of the second order were not observed experimentally. In all known cases the temperature dependence $[\partial\sigma_{GB}/\partial T - \partial(2\sigma_{SL})/\partial T]$ has a discontinuity of first derivative in temperature dependence of the Gibbsian energy of the interface/interfaces separating two adjacent grains at T_w. The $\theta(T)$ dependence is in all cases convex (like those shown in Fig. 2 for the Zn–Sn system) and follows the $\theta \sim \tau^{1/2}$ law (see example in Fig. 5 for the Al–Sn system).

At T_w the *tie-line of the GB wetting phase transition* appears in the two-phase region $(S + L)$ of the bulk phase diagram (the Zn–Sn phase diagram in Fig. 3). Above this tie line GBs with an energy σ_{GB} cannot exist in equilibrium with the liquid phase. The liquid phase forms a layer separating the crystals. In Fig. 3 two GB

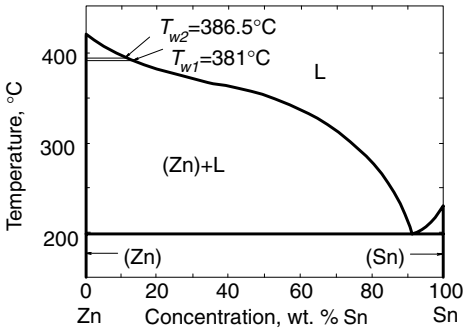

Figure 3. The Zn–Sn phase diagram. Thick lines represent the bulk phase transitions [37]. Thin lines at $T_{w2} = 386.5$°C and $T_{w1} = 381$°C are the tie-lines of the GB wetting phase transitions in the (Zn) + L two phase area (see also Fig. 2) [7].

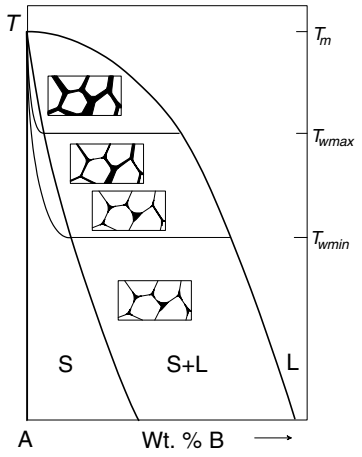

Figure 4. Scheme of the phase diagram with lines of bulk and GB phase transitions. Thick lines represent the bulk phase transitions. Thin lines represent the tie-lines of the GB wetting phase transition in the $S+L$ area for the high angle GBs having maximal and minimal possible energy and the GB premelting phase transition in the solid solution area S.

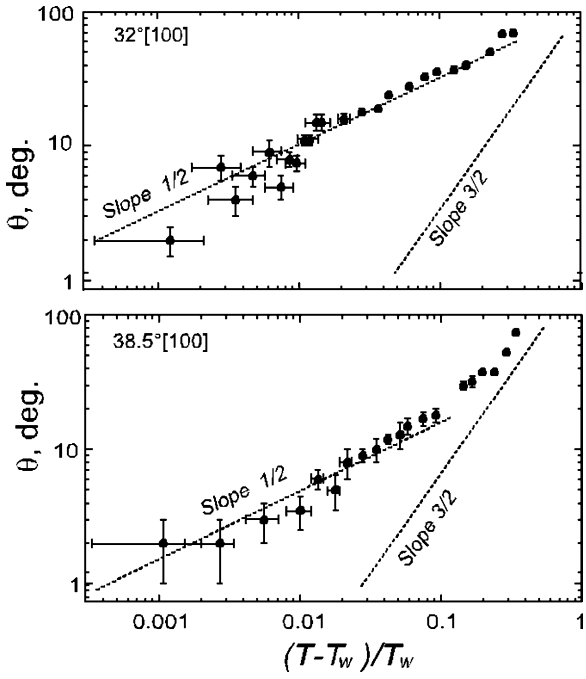

Figure 5. Dependence of contact angle θ from $(T - T_w)/T_w$ for two tilt [100] GBs in the Al–Sn system [18]. Dotted lines have the slope 1/2 and 3/2 corresponding to the phase transitions of 1st and 2nd order.

wetting tie lines are shown for two GBs with different energies obtained by measurements of $\theta(T)$ dependencies (Fig. 2). In polycrystals the whole spectrum of GBs exist with various energies. Therefore, in polycrystals the maximal $T_{w\max}$ and minimal $T_{w\min}$ can be found for high-angle GBs with minimal and maximal energy σ_{GBmin} and σ_{GBmax}, respectively. The tie-lines at $T_{w\max}$ and $T_{w\min}$ are shown in the schematic phase diagram (Fig. 4). At the temperature between $T_{w\max}$ and $T_{w\min}$ some GBs are wetted by the liquid phase and other GBs are not wetted. In this case the non-diffusional penetration of the liquid phase into the polycrystal would proceed inhomogenously. Such inhomegenous penetration of liquid phase (Ni) into *W* polycrystals was observed in [29]. With increasing temperature between $T_{w\max}$ and $T_{w\min}$ the fraction of the wetted GBs increase from 0 at $T_{w\min}$ to 100% at $T_{w\max}$.

First indications of the GB wetting phase transitions were found by measuring the contact angles in polycrystals [17]. Correct measurements were later perfomed using metallic bicrystals with individual tilt GBs in the Al–Sn (Fig. 5), Cu–In [4], Al–Pb–Sn [3, 18, 19], Al–Ga, Al–Sn–Ga [20, 21], Cu–Bi [5, 22, 23, 30], Fe–Si–Zn [24–27], Mo–Ni [28], W–Ni [29] and Zn–Sn (Figs. 2 and 3) [7] systems. The tie-lines of the GB wetting phase transition were constructed basing on the experimental data [3, 4, 7, 18–29]. The difference in the GB wetting phase transition temperature was experimentally demonstrated for GBs with different energies [4, 18]. Precise measurements of the temperature dependence of the contact angle revealed also that the GB wetting phase transition is of the first order [18]. The indications for the presence of the liquid-like phase along the dislocation lines were also found [23].

Grain Boundary Prewetting (Premelting) Phase Transitions

It was pointed out by Cahn [31] that, when the critical point is approached, where the difference between two phases disappears, two phases GBs of one critical phase should be wetted by a layer of another critical phase, and in the one-phase region of a phase diagram there should be a singularity connected with an abrupt transition to a microscopic wetting layer. We distinguish two possible situations: the first one, when a layer of the new phase is formed on the GB (*prewetting transition*), and the second one, when the GB is replaced by a layer of the new phase (*premelting phase transition*). At the prewetting transition the difference between two phases must be small, while at the premelting

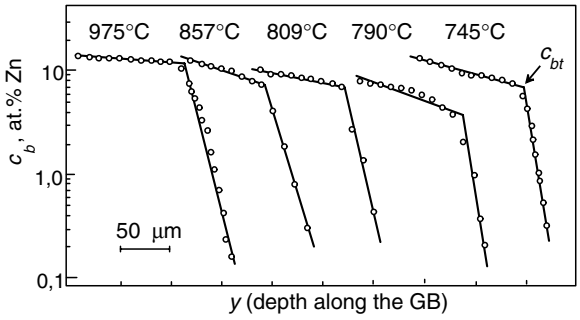

Figure 6. Dependences of the GB Zn concentration c_b after diffusion into the GBs in Fe—5 at. Si bicrystals on the depth y in Fisher's coordinates lg $c_b - y$ at various temperatures [24]. All these curves possess the high-$D_b\delta$ part (with low slope) and low-$D_b\delta$ part (with high slope). The $D_b\delta$ changes abruptly at their intersection c_{bt}.

transition the wetting phase may differ from that of the bulk dramatically. The lines of the GB prewetting or premelting phase transitions appear in the one-phase areas of the bulk phase diagrams where only one bulk phase can exist in the thermodynamic equilibrium (e.g. solid solution S, see Fig. 4). These lines continue the tie-lines of the GB wetting phase transitions and represent the GB solidus (Fig. 4). The thin liquid-like layer of the GB phase exists on the GBs between the bulk solidus and GB solidus in the phase diagram. During the GB premelting phase transition this layer appears abruptly on the GB by the intersection of GB solidus. As a result, the GB properties (diffusivity, mobility, segregation) change dramatically.

In other words, above the GB wetting tie-line T_w in the $S + L$ area of the bulk phase diagram $\sigma_{GB} > 2\sigma_{SL}$. Let us intersect the bulk solidus at $T = \text{const}$ and move into the one-phase area S of the bulk phase diagram. The GB energy σ_{GB} in the one-phase region close to the bulk solidus is still higher that the energy $2\sigma_{SL}$ of two solid-liquid interphase boundaries. Therefore, the GB still can be substituted by two solid-liquid interfaces, and the energy gain $\Delta G = \sigma_{GB} - 2\sigma_{SL}$ appears by this substitution. ΔG permits to stabilize the GB layer of the liquid-like phase. The appearance of the liquid-like phase (otherwise unstable in the bulk) between two S/L interfaces instead of the GB leads to the energy loss Δg per unit thickness and unit square. Therefore, the GB layer of the liquid-like phase has the thickness l defined by the equation $\sigma_{GB} - 2\sigma_{SL} = \Delta g l$. The thickness l depends on the concentation and temperature and becomes $l = 0$ at the line of GB premelting (or prewetting) phase transition.

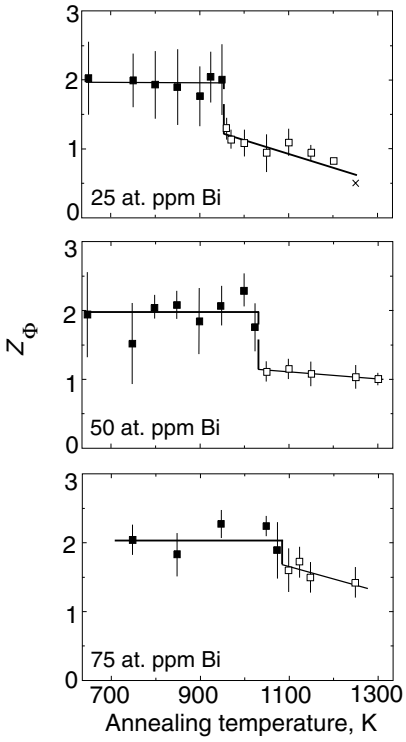

Figure 7. Temperature dependence of the GB Gibbsian excess Z_Φ of Bi in Cu(Bi) polycrystals of various compositions, measured by AES [5, 23, 33, 34].

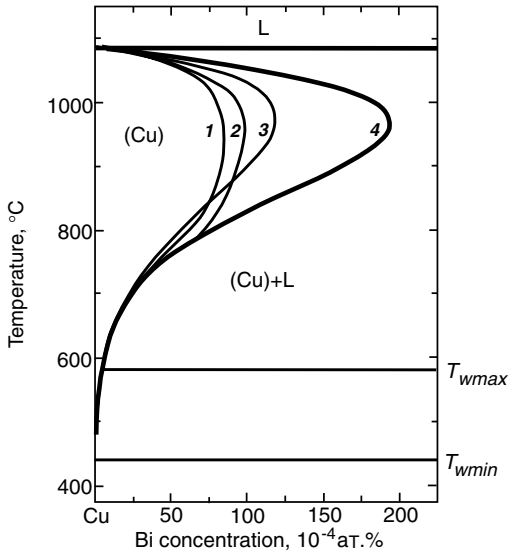

Figure 8. Cu–Bi phase diagram. Curves 1 and 2 are the GB solidus lines obtained on two different individual tilt GBs [35]. Curve 3 is the GB solidus line obtained on the Cu—Bi polycrystals [5, 23, 33]. Curve 4 is the (retrograde) bulk solidus line [22]. The GB wetting phase transition tie-lines at $T_{w\max}$ and $T_{w\min}$ are also shown in the two-phase $S + L$ area.

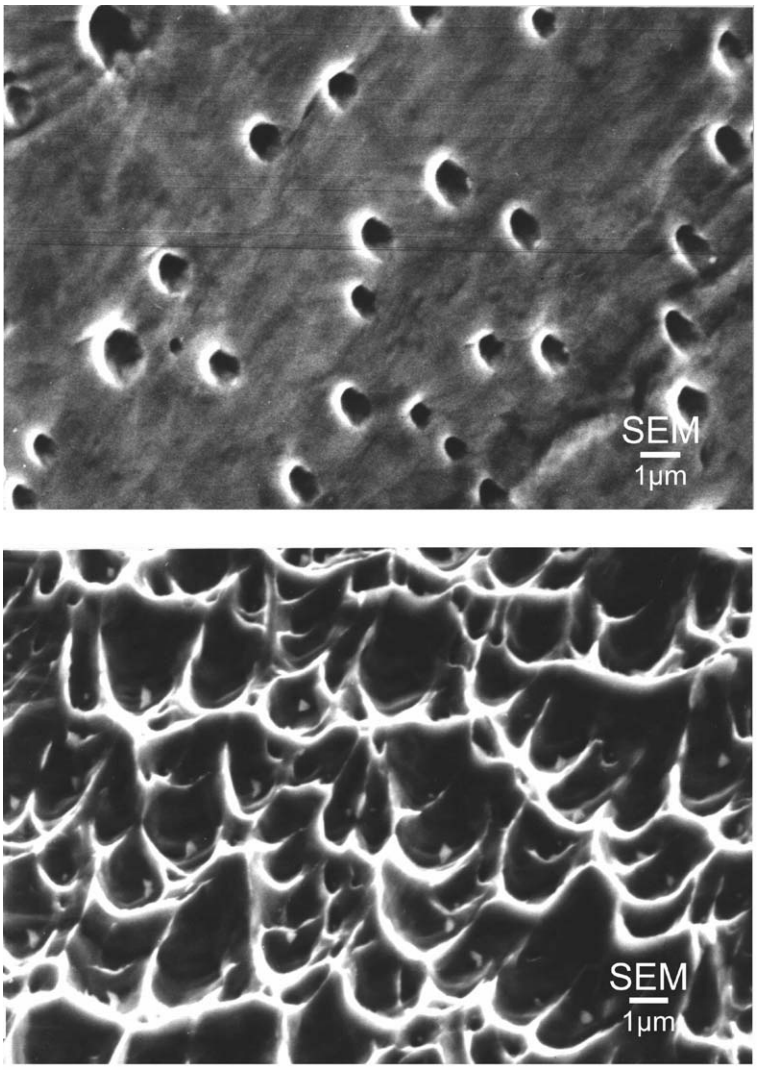

Figure 9. Micrographs of the GB fracture surfaces for two Cu bicrystals containing $100 \cdot 10^{-4}$ at.% Bi with tilt GBs 36.5° ⟨001⟩ and 33.2° ⟨001⟩. (a) 36.5° ⟨001⟩, 800°C, $Z^{\Phi} = 1$ ML. (b) 33.2° ⟨001⟩, 900°C, $Z^{\Phi} = 2$ ML.

The premelting transition has been revealed in the ternary Fe—Si—Zn system by measurements of Zn GB diffusivity along tilt GBs in the Fe—Si alloys [24–27]. It was found that the penetration profiles of Zn along GBs consist of two sections (Fig. 6), one with a small slope (high GB diffusivity $D_b\delta$) at high Zn concentrations and one with a large slope (low GB diffusivity) at low Zn concentrations. The transition from one type of behavior to the other was found to occur at a definite Zn concentration c_{bt} at the GB, which is an equilibrium characteristic of a GB and depends on the temperature and pressure (Fig. 6). The GB diffusivity increases about two orders of magnitude which is an indication of a quasi-liquid layer present in the GBs at high Zn concentration. The line of GB premelting phase transition in the one-phase area of the bulk phase diagram continues the line of the GB wetting phase transion in the two-phase $L + S$ area: by pressure increase both the GB wetting and the GB enhanced diffusivity disappear together at the same pressure value [27].

The *GB mobility* was studied for two tilt GBs in bicrystals grown of high purity 99.999 wt.% Al and of the same material doped with 50 wt. ppm Ga [21].

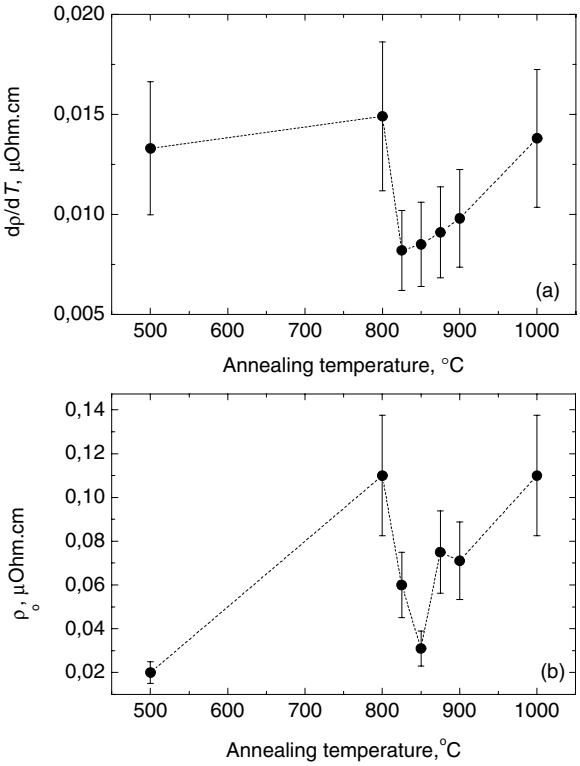

Figure 10. (a) Dependence of the temperature derivative of the resistivity $d\rho/dT$ and (b) residual resistivity ρ_0 of the Cu-75 at. ppm Bi polycrystals on the annealing temperature [34].

The GB mobility increased about 10 times by addition of Ga for the both GBs studied. Normally, the addition of a second component can only decrease the GB mobility due to the solute drag [32, 45, 46]. The increase of the GB mobility can be also explained by the formation of the liquid-like Ga-rich layer on the GBs as a reslut of a premelting phase transition.

The *GB segregation* of Bi in Cu was studied in the broad temperature and concentration interval [5, 22, 23, 33, 34]. It was shown that at a fixed Bi concentration the GB segregation Z_Φ changes abruptly at a certain temperature (Fig. 7). Below this temperature the GB Bi concentration is constant and corresponds to a thin layer of pure Bi (GB phase). Above this temperature the GB segregation is lower than one monolayer of Bi and decreases gradually with increasing temperature according to the usual laws. These features indicate also the formation of a thin layer of a GB phase in the one-phase area of the bulk Cu—Bi phase diagram (Fig. 8). The points of the abrupt change of the GB segregation form the GB solidus line in the bulk Cu—Bi phase diagram [22, 23, 33, 34]. GB segregation was measured with the aid of Auger electron spectroscopy (AES) on the GB fracture surfaces in samples broken *in situ* in the AES instrument. In other words, the multilayer GB segregation in Cu—Bi alloys leads to the increased *GB brittleness*. In Fig. 9 the microstructure of GB fracture surfaces is shown for two individual GBs with and without quasi-liquid layer of GB phase (after quenching, samples were broken *in situ* in the AES instrument). In Fig. 8 the (retrograde) bulk solidus line (Curve 4 [22]) is shown together with the GB solidus line obtained on the Cu—Bi polycrystals (Curve 3 [5, 23, 33]) and on two different individual tilt GBs (Curves 1 and 2 [35]). The GB wetting phase transition tie-lines at $T_{w\max}$ and $T_{w\min}$ are also shown in the two-phase $S + L$ area. Both latter lines were constructed using the data on fraction of wetted GBs (Fig. 6 [30]). The GB solidus lines (Curves 1, 2 and 3) lie completely in the one-phase S area of the Cu—Bi bulk phase diagram. The lines of individual GBs (Curves 1 and 2) intersect the GB solidus for the polycrystals. This is due to the fact that the GB fracture in the polycrystals "chooses" the most brittle GBs, which are different at different temperatures. Ii is also clearly seen that the GB solidus lines are positioned completely above the GB wetting tie-lines. Therefore, the GB solidus lines in the one phase S area of Cu–Bi phase diagram can be considered as continuation of the GB wetting tie-lines in $S + L$ two-phase area. In [36] the GB energy was measured in Cu–Bi alloys using individual $\Sigma 19$ GB in bicrystals with the aid of the GB thermal grooves. The thermal groove profile was obtained with the aid of atomic force microscopy. The GB Bi segregation was measured simultaneously in the same conditions. The abrupt change of the segregation coincides with the *discontinuity of first derivative in the temperature dependence of the Gibbsian energy of the interface/interfaces separating two adjacent grains.* This fact demonstrates that the GB premelting (or prewetting) phase transition is of first order. The low-temperature measurements of resistivity temperature coefficient $d\rho/dT$ and residual resistivity ρ_0 at 4 K were performed in [34] using the Cu—Bi polycrystals annealed at high temperature and subsequently quenched (Fig. 10). Both $d\rho/dT$ and ρ_0 demonstrate well pronounced break exactly at the same position where the sudden change of GB segregation was observed. In other words, the formation of GB layers of liquid-like phase leads to the measurable changes of *resistivity*.

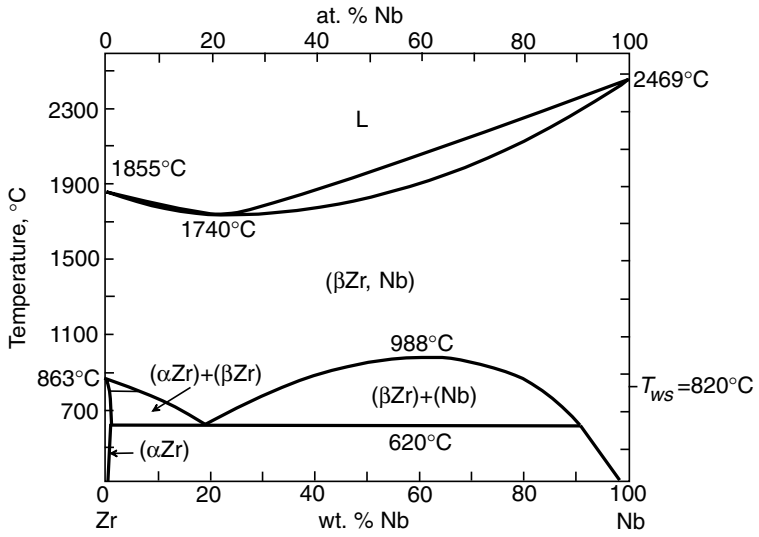

Figure 11. Phase diagram Zr—Nb with lines of the bulk phase transitions (thick solid lines [37]) and the tie-line of the GB covering phase transition at 820°C (thin solid line).

Grain Boundary Wetting (Covering) by Solid Phase

The situation illustrated in Fig. 1 can repeat in case if the second phase (β) is not liquid but also solid. In other words, if in the phase α the GB energy $\sigma_{\alpha\alpha}$ is lower that the energy of two α/β solid/solid interfaces, the GB $\alpha\alpha$ has to be substituted by the layer of the second solid phase β. Such process can be called the GB wetting (or covering) by solid phase. It is clear, that the kinetics of the equlibration processes in case of GB wetting (or covering) by a solid phase is much slower than in case of wetting by liquid phase. Our preliminary experiments with Al—95 wt.% Zn alloy demonstrate that after about 1 month of annealing the difference in the morphology of Al-rich phase precipitates (Al) at the (Zn)/(Zn) GBs in Zn-rich phase can be observed. Namely, at high temperatures just below the eutectic temperature in the Al—Zn system, more than 50% of (Zn)/(Zn) GBs are covered by continuous layer of the Al-rich phase. With decreasing temperature the portion of the (Zn)/(Zn) GBs covered by the (Al) layer decreased, and at the temperatures just below the eutectoid point all (Al) precipitates at the (Zn)/(Zn) GBs have the shape of isolated particles. Another examples of the GB covering phase transitions can be found by the analysis of the data published in the literature. In Fig. 11 the phase diagram Zr—Nb is shown. Thick solid lines represent the bulk phase transitions

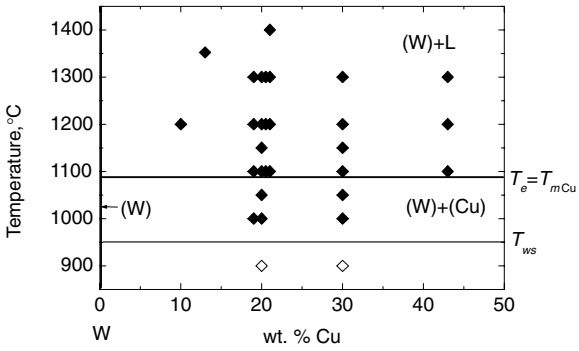

Figure 12. Phase diagram W—Cu with lines of the bulk phase transitions (thick solid lines [37]) and the tie-line of the GB covering phase transition at 950°C (thin solid line). The experimental points correspond to the two different GB morphologies in the W—Cu polycrystals [39–44]. Solid squares: GBs in *W* are wetted by the layers of liquid (Cu) phase or covered by the solid (Cu) phase. Open squares: GBs in *W* are not covered by the solid (Cu) phase.

[37]. The thin solid line represents the tie-line of the GB covering phase transition at 820°C. Above this line the high-temperature (β-Zr, Nb) phase forms the continuous thick layers in the α-Zr GBs [38]. In Fig. 12 the W—Cu phase diagram is shown with lines of the bulk phase transitions (thick lines [37]) and the tie-line of the GB covering phase transition at 950°C (thin line). The experimental points correspond to the two different GB morphologies in the W—Cu polycrystals obtained

by liquid phase sintering or activated sintering [39–44]. Solid squares correspond to the GBs in W which are wetted by the layers of liquid (Cu) phase or covered by the solid (Cu) phase. Open squares denote the GBs in W which are not covered by the solid (Cu) phase.

Conclusions

The GB phase transitions can be observed both in two-phase and one-phase areas of bulk phase diagrams. In the two-phase $S + L$ area where solid and liquid phases are in equilibrium the GB wetting phase transition can take place at T_w. Above T_w the GB disappears being substituted by two solid/liquid interfaces and the (macroscopically thick) layer of the liquid phase. The tie-lines of the GB wetting phase transition must have a continuation (GB solidus) in the one-phase S area of the bulk phase diagram. By intersection of GB solidus line the GB prewetting or premelting phase transition proceeds. Between the lines of GB and bulk solidus the grain boundary is substituted by two solid/liquid interfaces and the thin layer of the liquid-like phase. This liquid-like phase is stable in the GB and unstable in the bulk. The liquid-like phase is stabilized in the GB due to the energy gain which appears as a result of substitution of the GB by two solid/liquid interfaces. The GB wetting and prewetting (premelting) phase transitions observed up-to-date are of first order. If the GB energy is higher than the energy of two solid/solid interfaces, the GB solid state wetting (covering) phase transition can occur in a two-phase $S_1 + S_2$ area of the phase diagram.

Acknowledgments

The financial support of Russian Foundation for Basic Research and the Government of the Moscow district (contracts 01-02-97039 and 01-02-16473), Deutsche Forschungsgemeinschaft (contracts Gu 258/12-1 and Ba-1768/1-2), Copernicus programme of EU (contract ICA2-CT-2001-10008), Nato Linkage Grant PST.CLG.979375 and the German Federal Ministry for Education and Research (contract WTZ RUS 00/209) is acknowledged.

References

1. T.G. Langdon, T. Watanabe, J. Wadsworth, M.J. Mayo, S.R. Nutt, and M. E. Kassner, Mater. Sci. Eng. A **166**, 237 (1993).
2. B.B. Straumal and W. Gust, Mater. Sci. Forum **207–209**, 59 (1996).
3. B. Straumal, D. Molodov, and W. Gust, J. Phase Equilibria **15**, 386 (1994).
4. B. Straumal, T. Muschik, W. Gust, and B. Predel, Acta Metall. Mater. **40**, 939 (1992).
5. L.-S. Chang, E. Rabkin, B.B. Straumal, S. Hofmann, B. Baretzky, and W. Gust, Defect Diff. Forum **156**, 135 (1998).
6. B. Straumal, V. Semenov, V. Glebovsky, and W. Gust, Defect Diff. Forum **143–147**, 1517 (1997).
7. B.B. Straumal, W. Gust, and T. Watanabe, Mater. Sci. Forum **294–296**, 411 (1999).
8. F. Ernst, M.W. Finnis, A. Koch, C. Schmidt, B. Straumal, and W. Gust, Z. Metallk. **87**, 911 (1996).
9. B.B. Straumal and L.S. Shvindlerman, Acta Metall. **33**, 1735 (1985).
10. E.L. Maksimova, L.S. Shvindlerman, and B.B. Straumal, Acta Metall. **36**, 1573 (1988).
11. J.W. Cahn, J. Chem. Phys. **66**, 3667 (1977).
12. S. Dietrich, in *Phase Transitions and Critical Phenomena*, edited by C. Domb and J. H. Lebowitz (Academic, London, 1988), vol. 12, p. 2.
13. D. Jasnov, Rep. Prog. Phys. **47**, 1059 (1984).
14. G. de Gennes, Rev. Mod. Phys. **57**, 827 (1985).
15. H. Kellay, D. Bonn, and J. Meunier, Phys. Rev. Lett. **71**, 2607 (1993).
16. J.W. Schmidt and M.R. Moldover, J. Chem. Phys. **79**, 379 (1983).
17. N. Eustathopoulos, L. Coudurier, J.C. Joud, and P. Desre, J. Crystal Growth **33**, 105 (1976).
18. B. Straumal, W. Gust, and D. Molodov, Interface Sci. **3**, 127 (1995).
19. B. Straumal, D. Molodov, and W. Gust, Mater. Sci. Forum **207–209**, 437 (1996).
20. B. Straumal, S. Risser, V. Sursaeva, B. Chenal, and W. Gust, J. Physique **IV 5-C7**, 233 (1995).
21. D.A. Molodov, U. Czubayko, G. Gottstein, L.S. Shvindlerman, B.B. Straumal, and W. Gust, Phil. Mag. Lett. **72**, 361 (1995).
22. L.-S. Chang, B.B. Straumal, E. Rabkin, W. Gust, and F. Sommer, J. Phase Equilibria **18**, 128 (1997).
23. L.-S. Chang, E. Rabkin, B. Straumal, P. Lejcek, S. Hofmann, and W. Gust, Scripta Mater. **37**, 729 (1997).
24. E.I. Rabkin, V.N. Semenov, L.S. Shvindlerman, and B.B. Straumal, Acta Metall. Mater. **39**, 627 (1991).
25. O.I. Noskovich, E.I. Rabkin, V.N. Semenov, L.S. Shvindlerman, and B.B. Straumal, Acta Metal. Mater. **39**, 3091 (1991).
26. B.B. Straumal, O.I. Noskovich, V.N. Semenov, L.S. Shvindlerman, W. Gust, and B. Predel, Acta Metall. Mater. **40**, 795 (1992).
27. B. Straumal, E. Rabkin, W. Lojkowski, W. Gust, and L.S. Shvindlerman, Acta Mater. **45**, 1931 (1997).
28. E. Rabkin, D. Weygand, B. Straumal, V. Semenov, W. Gust, and Y. Bréchet, Phil. Mag. Lett. **73**, 187 (1996).
29. V.G. Glebovsky, B.B. Straumal, V.N. Semenov, V.G. Sursaeva, and W. Gust, High Temp. Mater. Proc. **13**, 67 (1994).
30. I. Apykhtina, B. Bokstein, A. Khusnutdinova, A. Peteline, and S. Rakov, Def. Diff. Forum **194–199**, 1331 (2001).
31. J.W. Cahn, J. Phys. Colloq. **43-C6**, 199 (1982).
32. D. Weygand, Y. Bréchet, E. Rabkin, B. Straumal, and W. Gust, Phil. Mag. Lett. **76**, 133 (1997).

33. L.-S. Chang, E. Rabkin, B.B. Straumal, B. Baretzky, and W. Gust, Acta Mater. **47**, 4041 (1999).
34. B. Straumal, N.E. Sluchanko, and W. Gust, Def. Diff. Forum **188–190**, 185 (2001).
35. B.B. Straumal, S.I. Prokofjev, L.-S. Chang, N.E. Sluchanko, B. Baretzky, W. Gust, and E. Mittemeijer, Def. Diff. Forum **194–199**, 1343 (2001).
36. J. Schölhammer, B. Baretzky, W. Gust, E. Mittemeijer, and B. Straumal, Interf. Sci. **9**, 43 (2001).
37. T.B. Massalski et al. (eds.), *Binary Alloy Phase Diagrams* (ASM International, Materials Park, 1993).
38. M.J. Iribarren, O.E. Agüero, and F. Dyment, Def. Diff. Forum. **194–199**, 1211 (2001).
39. Ya.E. Geguzin, *Physics of Sintering*, 2nd edition (Nauka, Moscow, 1984) (in Russian).
40. V.N. Eremenko, Yu.V. Naidich, and I.A. Lavrinenko, *Sintering in the Presence of Liquid Phase* (Naukova Dumka, Kiev, 1968) (in Russian).
41. V.V. Panichkina, M.M. Sirotjuk, and V.V. Skorokhod, Poroshk. Metall. **6**, 21 (1982) (in Russian).
42. V.V. Skorokhod, V.V. Panichkina, and N.K. Prokushev, Poroshk. Metall. **8**, 14 (1986), (in Russian).
43. V.V. Skorokhod, Yu.M. Solonin, N.I. Filippov, and A.N. Poshin, Poroshk. Metall. **9**, 9 (1983) (in Russian).
44. W.J. Huppmann and H. Riegger, Acta Metall. **23**, 965 (1975).
45. G. Gottstein and L.S. Shvindlerman, *Grain Boundary Migration in Metals* (Boca Raton etc., CRC Press, 1999).
46. H. Gleiter and B. Chalmers, *High-Angle Grain Boundaries* (Oxford etc., Pergamon Press, 1972).